Mössbauer characterisations and magnetic properties of iron cobaltites CoxFe3−xO4 (1 ≤ x ≤ 2.46) before and after spinodal decomposition

Hoa Le Trong, Lionel Presmanes, Eddy de Grave, Antoine Barnabé, Corine Bonningue, Philippe Tailhades

Mössbauer characterisations and magnetic properties of iron cobaltites $Co_xFe_{3-x}O_4$ ($1 \leq x \leq 2.46$) before and after spinodal decomposition

H. Le Trong [a,b], L. Presmanes [a,*], E. De Grave [c], A. Barnabé [a], C. Bonningue [a], Ph. Tailhades [a]

[a] Université de Toulouse, UPS, INP, Institut Carnot CIRIMAT UMR CNRS 5085, 118, Route de Narbonne, F-31062 Toulouse Cedex 9, France
[b] Faculty of Chemistry, University of Sciences, Vietnam National University HoChiMinh City, 227 Nguyen Van Cu, Q 5, 769999 HoChiMinh, Viet Nam
[c] NUMAT, Department of Physics and Astronomy, University of Ghent, Proeftuinstraat 86, B-9000 Gent, Belgium

* Corresponding author. Fax: +33 561556163.
E-mail address: presmane@chimie.ups-tlse.fr (L. Presmanes).

A B S T R A C T

Iron cobaltite powders $Co_xFe_{3-x}O_4$ ($1 \leq x \leq 2.46$) were synthesized with compositions in between the cobalt ferrite $CoFe_2O_4$ and $Co_{2.46}Fe_{0.54}O_4$. The cationic distribution of pure spinel phases was determined by Mössbauer spectroscopy: as Co content increases in the spinel oxide, Co^{3+} cations replace Fe^{3+} cations in the octahedral sites and Co^{2+} cations migrate from octahedral to tetrahedral sites. Saturation magnetizations M_S measured at 5 K by a SQUID magnetometer were consistent with the values calculated from the cationic distribution. M_S decreases as diamagnetic Co^{3+} cations replace strongly magnetic Fe^{3+} cations. Two spinel phases were formed by spinodal decomposition of $Co_{1.73}Fe_{1.27}O_4$ phase submitted to a subsequent thermal treatment, one with a high amount of iron $Co_{1.16}Fe_{1.84}O_4$ and one other containing mostly cobalt $Co_{2.69}Fe_{0.31}O_4$. Increase of the experimental M_S value obtained after the spinodal decomposition is in accordance with the calculated value deduced from the cationic distribution of the two phases.

Keywords:
Spinel oxide
Cobaltite
Mössbauer
Spinodal decomposition

1. Introduction

The spinodal decomposition is a phase segregation mechanism, which can occur in a miscibility gap of a phase diagram. This out of equilibrium process leads to pseudo-periodic distribution of the precipitated phases when interrupted before end. Materials with alternate nanometric layers of different phases can then be created. As a result, the spinodal decomposition is then a way to obtain self-organised materials which could display original properties. For instance, giant magnetoresistance (GMR) property was already revealed for metallic alloys after their spinodal transformation [2–4]. Other collective properties, such as magnetic band gap effects [1] could be also observed in these types of nanostructured materials.

Spinel iron cobaltites $Co_xFe_{3-x}O_4$ with x in between 1.1 and 2.7 are located inside the miscibility gap of the Fe_3O_4–Co_3O_4 phase diagram [5–9] and can then be submitted to spinodal decomposition when heat treated for several hours at about 500–700 °C [7,8]. In a previous work carried out on cobaltite powders [10] we specified the preparation conditions required to obtain the best-suited periodic structures and we observed the stacking-up of alternate nanometric areas of cobalt-rich and iron-rich spinel phases. The periodicity of the nanostructuration of the material was estimated to be close to nm.

Mössbauer spectroscopy and magnetic measurements were already done on iron cobaltites [13,16,20,23,24]. Cationic distributions were proposed from these works. However, the location of the cations in the spinel lattice, strongly depends on the thermal history of the samples and it is also greatly influenced by the spinodal transformation. This work is then focused on the determination on the cationic distribution for iron cobaltites prepared in well controlled conditions, on the one hand, and on the characterization of the spinodal transformation in one selected sample corresponding to $Co_{1.73}Fe_{1.27}O_4$, on the other hand. This oxide was selected because it displays a chemical composition within the miscibility gap of the Fe_3O_4–Co_3O_4 phase diagram. It was studied before (quenched from 900 °C), during (36 h at 700 °C) and after (120 h at 700 °C) the spinodal transformation.

2. Experimental

Oxalate precursors $(Co_xFe_{3-x})_{1/3}C_2O_4 \cdot 2H_2O$ were synthesized according to the previously described 'chimie douce' method [10]. Iron (II) chloride tetrahydrate $FeCl_2 \cdot 4H_2O$ and cobalt (II) chloride hexahydrate $CoCl_2 \cdot 6H_2O$ were weighted in the appropriate Co/Fe molar ratio to obtain $x = 1.00$, 1.22, 1.73, and 2.46. The oxalate powders were decomposed in air at 600 °C, heated to 900 °C and then quenched to room temperature to get monophase iron cobaltite $Co_xFe_{3-x}O_4$. Two examples of Scanning Electron Microscopy (SEM) images of the oxalate and the oxide for the composition $x = 1.73$ are shown in Fig. 1a and b respectively.

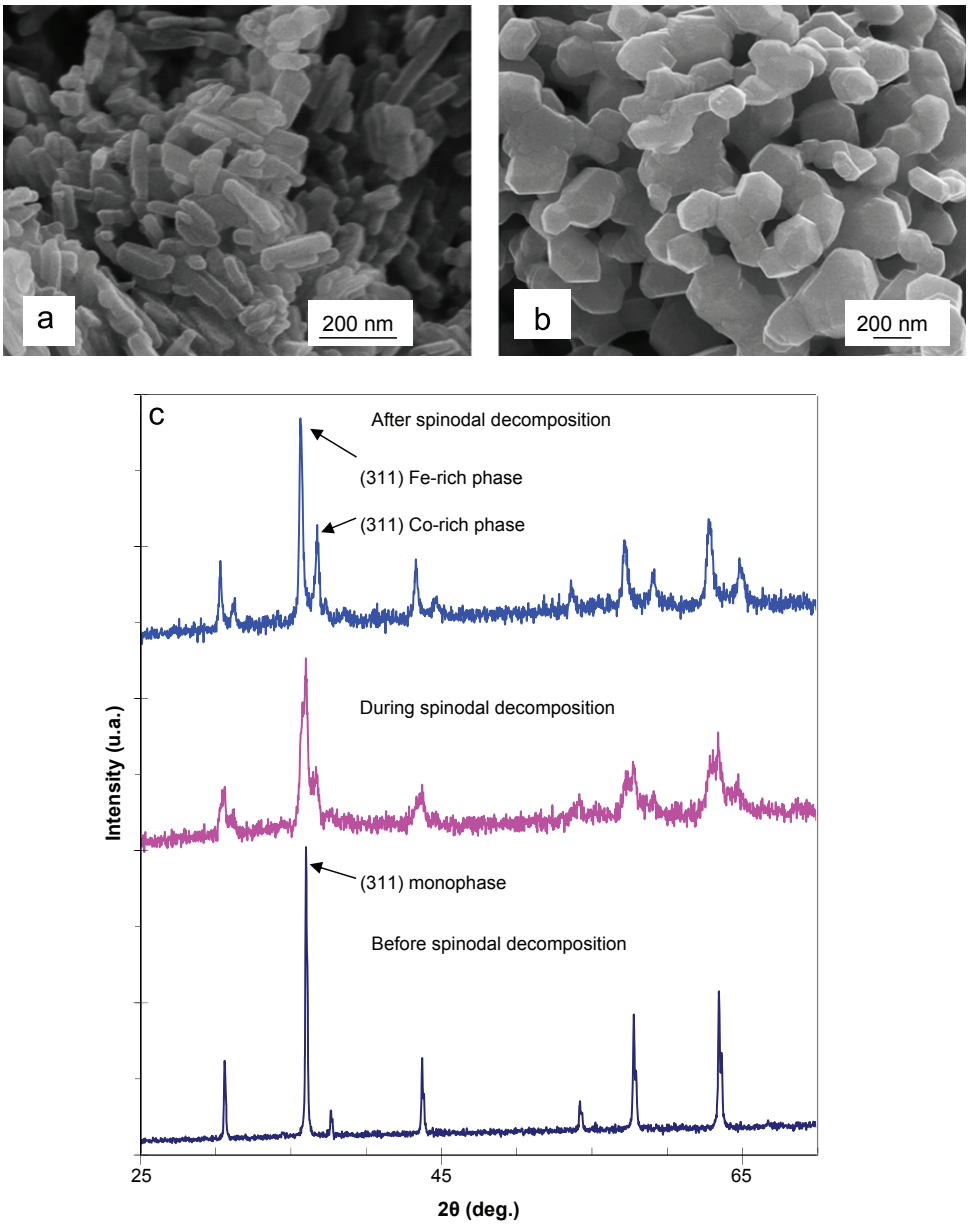

Fig. 1. SEM images of (a) oxalate $(Co_{1.73}Fe_{1.27})_{1/3}C_2O_4 \cdot 2H_2O$ and (b) oxide $Co_{1.73}Fe_{1.27}O_4$ and (c) XRD pattern of $Co_{1.73}Fe_{1.27}O_4$ powder quenched at 900 °C and annealed at 700 °C 36 h and 120 h.

The purity of the phases and the lattice parameters were determined by powder X-ray diffraction (XRD) using a Bruker D4 Endeavor X-ray diffractometer. Copper radiation was used as the X-ray source ($\lambda(Cu_{k\alpha 1})=1.5405$ Å and $\lambda(Cu_{k\alpha 2})=1.5445$ Å). XRD patterns were refined by the Rietveld method implemented in the Fullprof/WinPlotR software package [11].

Mössbauer spectra (MS) in transmission geometry were collected at room temperature (RT) and at 5 K. A spectrometer operating in constant acceleration mode with triangular reference signal and a ^{57}Co (Rh) source were used. Accumulation of the data was performed in 1024 channels using the WISSEL CMCA-550 unit and continued until a background of 10^6 counts was reached. The spectrometer was calibrated by collecting the spectrum of a standard α-Fe_2O_3 powder at RT. Isomer shift data quoted hereafter are with respect to α-Fe at RT.

Mössbauer measurements had to be performed in external magnetic fields to enhance the separation of the sub-spectra due to octahedral and tetrahedral Fe species, respectively. An external field of 60 kOe parallel to the direction of the incident γ-rays was applied at 5 K. For these measurements the calibration spectra were recorded simultaneously using another source and counting electronics at the opposite end of the transducer. The field was applied before the samples were cooled down, using liquid helium, in order to simulate the measuring conditions of the SQUID measurements.

Magnetic measurements were done at 5 K with a superconducting quantum interference device (SQUID) magnetometer MPMS quantum design 5.5 in a maximum applied field of 40 kOe.

3. Results and discussion

3.1. Study of monophased cobaltites $Co_xFe_{3-x}O_4$ $(1 \le x \le 2.46)$

In a previous work [10], the authors have shown from an XRD study that pure spinel phases were obtained for samples annealed

at 900 °C and subsequently quenched, whatever the value of x. As an example, the XRD pattern of the phase with a composition $x=1.73$ is presented in Fig. 1c. The lattice constant of the iron cobaltites decreases with the increase of the cobalt content due to the replacement of high-spin Fe^{3+} octahedral ion [$r(Fe^{3+})_{VI}\sim0.785$ Å] by low-spin Co^{3+} with the same coordination [$r(Co^{3+})_{VI}\sim0.685$ Å] [12]. The values of the lattice constants vary in between the corresponding parameters of $CoFe_2O_4$ and Co_3O_4.

Mössbauer spectra of these powders, acquired at room temperature (RT) without external magnetic field are presented in Fig. 2. The iron cobaltites with the composition $x=1.00$, 1.22, and 1.73 are ferrimagnetic and are essentially composed of two more or less strongly overlapping sextets related to the presence of iron in tetrahedral sites (A-sites) and octahedral sites (B-sites). For the cobalt-rich sample ($Co_{2.46}Fe_{0.54}O_4$), the RT Mössbauer spectrum consists of a doublet with a quadrupole splitting of ~0.53 mm/s, an isomer shift of 0.32 mm/s and a line width of 0.32 mm/s. At RT, this oxide is thus purely paramagnetic. This result is in agreement with the magnetic data related to iron cobaltites published by Robin [5] and Takahashi and Fine [13] showing that the Curie temperature (T_c) decreases when the cobalt content increases. For the composition $Co_{2.46}Fe_{0.54}O_4$, T_c is below RT and thus this oxide is paramagnetic. Two other Mössbauer measurements for the $x=2.46$ sample (not shown) were subsequently carried out at 140 K and 170 K. In the spectrum obtained at 170 K, the doublet is still present. However, the spectrum measured at 140 K exclusively shows a broad unresolved sextet. Consequently, the Curie temperature for the involved composition is in between 140 K and 170 K. This range is lower than the value ($T_c\sim220$ K) deduced from the curve proposed by Takahashi and Fine [13], which could be due to a difference in the cationic distribution as it will be argued in a forthcoming section.

Additional measurements were carried out at 5 K under a longitudinal external field H_{ext} of 60 kOe. The Mössbauer spectra collected were analyzed in terms of two model-independent distributions for the observed effective hyperfine fields, H_{eff}, acting at the A- and B-site ^{57}Fe probes, respectively. In general, the effective hyperfine field $\vec{H}_{eff}$ is given by $\vec{H}_{eff}=\vec{H}_{hf}+\vec{H}_{ext}$ and its magnitude, as directly measured from the external-field spectrum, depends on the angle between the hyperfine field $\vec{H}_{hf}$ and the external field $\vec{H}_{ext}$. Information about the direction of the hyperfine field acting at a given Fe-site with respect to that of the external field is obtained from the relative spectral areas $A_{i,7-i}$ of the absorption lines $i=1$–6 constituting the applied-field spectrum for that site. The angle θ, or $\pi-\theta$, the so-called *canting angle*, between the effective hyperfine field and the γ-ray direction, which in the present experiments coincides with the direction of the external field, is given by [14]

$$\theta=\arcsin\left[\frac{1.5(A_{2,5}/A_{1,6})}{1+0.75(A_{2,5}/A_{1,6})}\right]^{1/2},$$

in which $A_{2,5}/A_{1,6}$ is the ratio of the area of the middle absorption lines (lines 2 and 5 of the sextet spectrum) relative to the area of the outer absorption lines (lines 1 and 6). For most Fe^{3+}-bearing magnetic materials, the direction of the ferric hyperfine field $\vec{H}_{hf}$ is opposite to that of the atomic spin. Consequently, when for a given single-site Fe^{3+} compound subjected to an external field the atomic spins are ordered fully parallel to that external field (i.e., hyperfine field antiparallel and $\theta=180°$), then $H_{eff}=H_{hf}-H_{ext}$ and $A_{2,5}/A_{1,6}=0$, the latter condition meaning that the middle lines in the external-field spectrum of that compound are absent.

The observed and calculated applied-field spectra are reproduced in Fig. 3. It is noticed that for the oxides with cobalt contents $x=1.00$, 1.22, and 1.73 the two sextet sub-spectra arising from iron on A- and B-sites, respectively, are clearly shifted apart due to the external field. This effect is well known to occur in ferrimagnetic substances, whereby the individual spins of the sublattice with the larger net magnetic moment order parallel to the external field, and those of the sublattice with the smaller net magnetic moment antiparallel, so that for the former sublattice sites the external field subtracts from the hyperfine field, and for the latter ones the external field adds to the hyperfine field. For the present cobaltites, the alignment is not complete as evidenced by the presence of the middle absorption lines (lines 2 and 5) in the respective MS. This deviation from total alignment is generally due to the magnetic anisotropy, which forces the magnetic moment of a randomly oriented (with respect to the external

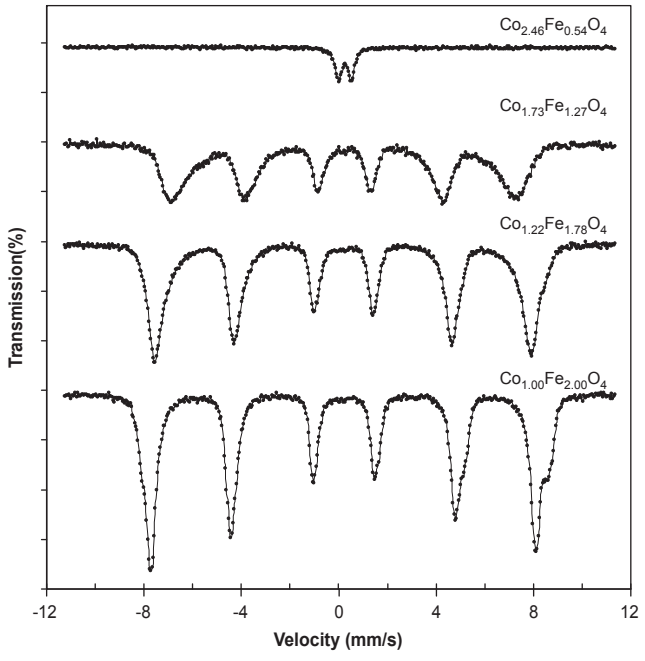

Fig. 2. RT Mössbauer spectra of $Co_xFe_{3-x}O_4$ powders ($1.00\le x\le2.46$) quenched at 900 °C.

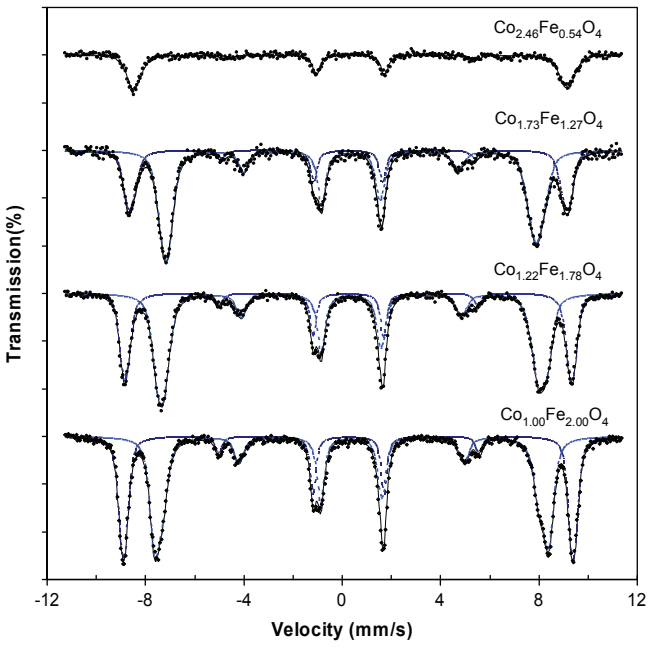

Fig. 3. Mössbauer spectra measured at 5 K with an applied magnetic field of 60 kOe for $Co_xFe_{3-x}O_4$ powders ($1.00\le x\le2.46$) quenched at 900 °C.

field) crystallite into a particular crystallographic direction within the crystallite. From Fig. 3 it is obvious that the relative spectral areas of the middle absorption lines decrease slightly with increasing Co content, implying that the magnetic anisotropy forces become weaker with increasing Co^{3+} for Fe^{3+} substitution. The external-field spectrum of the sample having $x=2.46$ (Fig. 3, top) consists of only four (broad) absorption lines. Qualitatively, this observation implies that the ferric cations exclusively occupy one particular kind of lattice site in the spinel structure (B-sites, see forthcoming discussion) and that their spins are perfectly aligned along the direction of the applied field.

Relevant Mössbauer parameters deduced from the applied-field spectra measured at 5 K are presented in Table 1. Within the experimental error limits, both A- and B-site quadrupole shifts (not shown) are zero for all compositions, which is common for most cubic spinel ferrites [14]. The isomer shifts are too small to be attributable to the presence of Fe^{2+} cations, but instead are typical for Fe^{3+} cations occupying A- and/or B-sites in spinel ferrites, i.e., 0.35–0.37 mm/s and 0.45–0.48 mm/s, respectively. Thus, on the basis of the obtained isomer-shift values, the sextet component with the highest effective hyperfine field can be attributed to A-site ferric species, and the sextet component with the lowest effective hyperfine field to B-site ferric species. Both effective hyperfine field values, H_{eff}, decrease with increasing Co^{3+} for Fe^{3+} substitution, which qualitatively can be explained by the diamagnetic nature of Co^{3+} cations. It should be noted at this point that the calculated H_{eff} values for the present $CoFe_2O_4$ sample (see Table 1, $x=1.0$) are very close to those obtained from the external-field spectrum (60 kOe, 4.2 K) of an earlier studied $CoFe_2O_4$ species as reported by de Bakker et al. [15], i.e., 566 kOe and 492 kOe for A- and B-sites, respectively, the small difference for the latter sites most likely being due to the different thermal history of the samples. Also the canting angle θ calculated from the observed $A_{2,5}/A_{1,6}$ area ratios for the present $CoFe_2O_4$ are very similar to those obtained by de Bakker et al. [15].

For sample $Co_{2.46}Fe_{0.54}O_4$ with low iron content, only one spectral component appears in the applied-field spectrum. The adjusted value for the isomer shift ($\sim$0.44 mm/s, see Table 1) irrefutably infers that this spectrum is due to Fe^{3+} species at the B-sites, which is consistent with the cationic distribution determined by Smith et al. [16] for the spinel $Co_{2.5}Fe_{0.5}O_4$. There are no significant contributions from the middle absorption lines. Hence, the parameter $A_{2,5}/A_{1,6}$ equals zero, implying that the corresponding ferric moments are directed along the external field, either

Table 1
Relevant Mössbauer parameters deduced from the spectra recorded at 5 K in an external magnetic field (60 kOe) for $Co_xFe_{3-x}O_4$ powders quenched at 900 °C; δ: isomer shift relative to α-Fe at room temperature; H_{eff}: maximum-probability effective hyperfine field; $A_{2,5}/A_{1,6}$: ratio of the area of the middle absorption lines (lines 2 and 5 of the sextet subspectrum) relative to the area of the outer absorption lines (lines 1 and 6); θ : angle between the direction of the effective hyperfine field and the γ-ray direction; H_{hf}: maximum-probability hyperfine field; R: subspectrum area relative to total spectral area.

x	A-sites						B-sites					
	δ (mm/s)	H_{eff} (kOe)	$A_{2,5}/A_{1,6}$	$\sin^2\theta$	H_{hf} (kOe)	R (%)	δ (mm/s)	H_{eff} (kOe)	$A_{2,5}/A_{1,6}$	$\sin^2\theta$	H_{hf} (kOe)	R (%)
1.00	0.364	566.3	0.113	0.156	511.7	39.9	0.491	497.0	0.167	0.223	550.6	60.1
1.22	0.356	563.7	0.109	0.151	508.9	35.1	0.466	473.1	0.162	0.217	526.9	64.9
1.73	0.353	553.6	0.098	0.137	498.4	31.3	0.467	467.5	0.152	0.205	521.7	68.7
2.46	–	–	–	–	–	–	0.444	550.0	–	–	490.0	100

Table 2
Cationic distribution of $Co_xFe_{3-x}O_4$ deduced from Mössbauer data.

Formula	Cationic distribution (present study)	Bibliographical data
$Co_{1.00}Fe_{2.00}O_4$	$Co^{2+}_{0.21}Fe^{3+}_{0.79}[Co^{2+}_{0.79}Fe^{3+}_{1.21}]O_4$	Sawatzky et al. [20]: ($x=1.00$) $Co^{2+}_{0.21}Fe^{3+}_{0.79}[Co^{2+}_{0.79}Fe^{3+}_{1.21}]O_4$ Ferreira et al. [23]: ($x=1.00$) $Co^{2+}_{0.23}Fe^{3+}_{0.77}[Co^{2+}_{0.77}Fe^{3+}_{1.23}]O_4$ Murray and Linnet [24]: ($x=1.04$) $Co^{2+}_{0.38}Fe^{3+}_{0.62}[Co^{2+}_{0.62}Fe^{3+}_{1.34}Co^{3+}_{0.04}]O_4$
$Co_{1.22}Fe_{1.78}O_4$	$Co^{2+}_{0.38}Fe^{3+}_{0.62}[Co^{2+}_{0.62}Fe^{3+}_{1.16}Co^{3+}_{0.22}]O_4$	
$Co_{1.73}Fe_{1.27}O_4$	$Co^{2+}_{0.61}Fe^{3+}_{0.39}[Co^{2+}_{0.39}Fe^{3+}_{0.88}Co^{3+}_{0.73}]O_4$	Murray and Linnet [24]: ($x=1.54$) $Co^{2+}_{0.58}Fe^{3+}_{0.42}[Co^{2+}_{0.42}Fe^{3+}_{1.04}Co^{3+}_{0.54}]O_4$
$Co_{2.00}Fe_{1.00}O_4$	Not studied in this work	Takahashi and Fine [13]: ($x=2.00$) $Co^{2+}_{0.6}Fe^{3+}_{0.4}[Co^{2+}_{0.4}Fe^{3+}_{0.6}Co^{3+}_{1.0}]O_4$ Murray and Linnet [24]: ($x=2.00$) $Co^{2+}_{0.7}Fe^{3+}_{0.3}[Co^{2+}_{0.3}Fe^{3+}_{0.7}Co^{3+}_{1.0}]O_4$ Smith et al. [16]: ($x=2.00$) $Co^{2+}_{0.55}Fe^{3+}_{0.45}[Co^{2+}_{0.45}Fe^{3+}_{0.55}Co^{3+}_{1.00}]O_4$ Ferreira et al. [23]: ($x=2.00$) $Co^{2+}_{0.46}Fe^{3+}_{0.54}[Co^{2+}_{0.54}Fe^{3+}_{0.46}Co^{3+}_{1.00}]O_4$
$Co_{2.46}Fe_{0.54}O_4$	$Co^{2+}_{1.00}[Fe^{3+}_{0.54}Co^{3+}_{1.46}]O_4$	Takahashi and Fine [13]: ($x=2.5$) $Co^{2+}_{0.8}Fe^{3+}_{0.2}[Co^{2+}_{0.2}Fe^{3+}_{0.3}Co^{3+}_{1.5}]O_4$ Murray and Linnet [24]: ($x=2.52$) $Co^{2+}_{0.96}Fe^{3+}_{0.04}[Co^{2+}_{0.04}Fe^{3+}_{0.44}Co^{3+}_{1.52}]O_4$ Smith et al. [16]: ($x=2.50$) $Co^{3+}_{1.0}[Fe^{3+}_{0.5}Co^{3+}_{1.5}]O_4$

antiparallel or parallel. Consequently, the hyperfine field H_{hf}, being opposite to the spin direction of the probe Fe^{3+} cations, is possibly given by $H_{hf}=H_{eff}-H_{ext}=490$ kOe or by $H_{hf}=H_{eff}+H_{ext}=610$ kOe. The latter possibility can be ruled out because such a high hyperfine field is close to the free-ion value for Fe^{3+} (630 kOe, see [17]) and has never been observed for any oxygen-based Fe-containing compound. From these qualitative considerations, it may be concluded that for sample $Co_{2.46}Fe_{0.54}O_4$ the Fe^{3+} cations are exclusively located at the octahedral sites in the spinel structure and that, in contrast to the cobaltites with the higher Fe contents, the sublattice magnetic moment for the A-sites is larger than that for the B-sites.

It has been argued that the recoilless fractions of ferric cations on octahedral and tetrahedral sublattices in a given spinel ferrite structure are equal within experimental error limits [18,19]. Consequently, the number of A- and B-site Fe^{3+} cations is to good approximation proportional to the respective relative spectral areas R observed in the Mössbauer spectrum. From the R values obtained for the present cobaltite samples (see Table 1), the cation distribution could thus be determined straightforwardly and the calculated formulas for all compositions are presented in Table 2, together with some literature data reported for similar compositions.

For cobalt ferrite $CoFe_2O_4$, the Co^{2+} cations have a strong preference for the octahedral sites, leading to an inverse structure. However, all earlier studies involving $CoFe_2O_4$ have shown that this ferrite exhibits a partially inverse structure, with inversion degree depending on the synthesis procedure. For example, Sawatzky et al. [20] showed by Mössbauer measurements at 100 K under 55 KOe external magnetic field, that the amount of Co^{2+} ions in tetrahedral sites can vary from 0.04 to 0.21 when the sample is respectively slowly cooled or quenched from 1200 °C. The cationic distribution determined by Mössbauer spectroscopy for the present $CoFe_2O_4$ sample agrees with that given for quenched samples by Sawatzky at al. [20].

When the amount of cobalt increases, the cell parameter decreases and there is a gradual evolution toward a normal spinel structure. The diamagnetic Co^{3+} cations replace the Fe^{3+} cations in the octahedral position and the octahedral preference of the Co^{2+} cations becomes less dominant. As mentioned above, for sample $Co_{2.46}Fe_{0.54}O_4$ all the iron is found in the octahedral position.

Cationic distributions of iron cobaltites $Co_xFe_{3-x}O_4$ ($1.00 < x < 2.46$) determined in this study by Mössbauer measurements agree well with the formulas

$$Co^{2+}_{\alpha}Fe^{3+}_{1-\alpha}[Co^{2+}_{1-\alpha}Fe^{3+}_{2-x+\alpha}Co^{3+}_{x-1}]O^{2-}_4 \quad (1 \le x \le 2,\ \alpha \le 1) \tag{1}$$

$$Co^{2+}_{x-2+\omega}Fe^{3+}_{3-x-\omega}[Co^{2+}_{3-x-\omega}Fe^{3+}_{\omega}Co^{3+}_{x-1}]O^{2-}_4 \quad (2 \le x \le 3,\ \omega \le 3-x) \tag{2}$$

given in our previous report and determined by X-ray diffraction and Poix's formula [10]. In other words, for $x=1.22$ and $x=2.46$ the structure formulas are: $Co^{2+}_{0.38}Fe^{3+}_{0.62}[Co^{2+}_{0.62}Fe^{3+}_{1.16}\ Co^{3+}_{0.22}]O^{2-}_4$ and $Co^{2+}_{1.00}[Fe^{3+}_{0.54}Co^{3+}_{1.46}]O^{2-}_4$ respectively.

Table 3 shows the sublattice magnetic moments M_A and M_B in unit Bohr magneton (μ_B) and the calculated saturation magnetization M_S taking into account the cationic distribution deduced from the Mössbauer spectra (Table 2). It has been assumed that the Co^{3+} cations are in a low-spin state and that their magnetization is zero. The magnetic moment of the Fe^{3+} cations was taken to be 5.0 μ_B and that for the high-spin Co^{2+} 3.2 μ_B as determined by Sawatzky et al. [21]. The total resulting saturation magnetization M_S can then easily be calculated according to the Néel model for a collinear ferrimagnetic material.

A comparison between calculated and measured magnetizations is presented in Fig. 4. The calculated values are in good agreement with the experimental results, except for sample $Co_{2.46}Fe_{0.54}O_4$ for which a slight deviation is observed. This feature can be due to the fact that a very small amount of iron, not detectable by the Mössbauer effect, remains located on the tetrahedral sites. The saturation magnetization of the cobaltites drastically decreases in going from $x=1$ to $x \approx 2.3$. For values of x higher than 2.3, the relative increase of the magnetic moment in the A sublattice due to increasing amount of diamagnetic Co^{3+} in B-sites makes the calculation by the collinear Néel model (solid line) less suitable. In particular Takahashi and Fine [13] showed from their low-temperature magnetization measurements of $Co_xFe_{3-x}O_4$ solid solutions that the real variation of M_S (dashed line) does not follow the Néel model for compositions above the compensation point. Similar results were found by Harrison and Putnis [22] for the system $(Fe_3O_4)_{1-x}$–$(MgAl_2O_4)_x$.

Values of saturation magnetization and cationic distribution of iron cobaltites will be taken as a reference later in this article, to deduce structural and magnetic properties of the two cobalt–iron oxides obtained at the end of spinodal decomposition.

Table 3
Number of Co and Fe cations per formula unit at the A and B sites in $Co_xFe_{3-x}O_4$ samples quenched at 900 °C as deduced from Mössbauer spectra, sublattice magnetic moments M_A and M_B in Bohr magneton μ_B and saturation magnetization M_S calculated according to the Néel model for a collinear ferrimagnetic material.

x	A-sites		B-sites			M_A (μ_B)	M_B (μ_B)	M_S (emu/g)
	Co^{2+} (3.2 μ_B)	Fe^{3+} (5 μ_B)	Co^{2+} (3.2 μ_B)	Fe^{3+} (5 μ_B)	Co^{3+} (0 μ_B)			
1.00	0.21	0.79	0.79	1.21	0.00	4.62	8.58	94.1
1.22	0.38	0.62	0.62	1.16	0.22	4.32	7.78	82.5
1.73	0.61	0.39	0.39	0.88	0.73	3.90	5.65	40.9
2.46	1.00	0.00	0.00	0.54	1.46	3.20	2.70	11.7

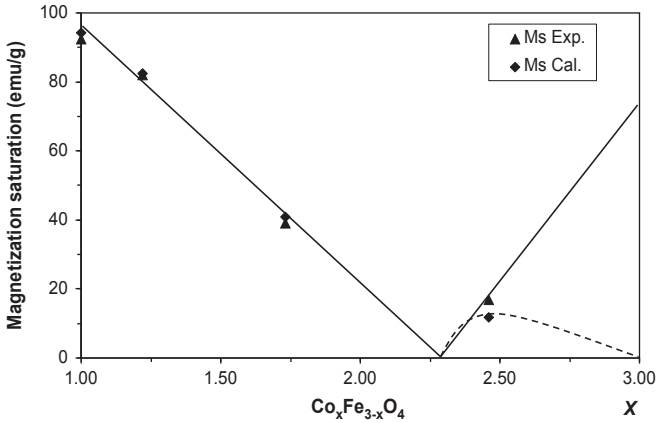

Fig. 4. Saturation magnetization (M_S) of $Co_xFe_{3-x}O_4$ ($x=1.00$, 1.22, 1.73, and 2.46) quenched at 900 °C, measured at 5 K and calculated at 0 K. The Néel model (solid line) is compared to the experimental results of Takahashi and Fine [13] (dashed line).

3.2. Study of $Co_{1.73}Fe_{1.27}O_4$ during and after spinodal decomposition

3.2.1. Sample annealed at 700 °C for 36 h (intermediate state of spinodal decomposition)

Annealing at 700 °C for 36 h was carried out on monophased $Co_{1.73}Fe_{1.27}O_4$ to promote spinodal decomposition. XRD pattern (Fig. 1c) shows contributions of three phases, the initial pristine phase and two new phases; one iron-rich (a=8.3552 Å, $x=1.23$) and one cobalt-rich ($a=8.1431$ Å, $x=2.61$). The formation of these

two new spinel phases leads to a small change of the lattice parameter of the initial single phase from 8.2861 Å to 8.2916 Å corresponding to a decrease of x from 1.73 to 1.65. The Mössbauer spectrum acquired at RT exhibits a doublet and a sextet due to the existence of these three phases in this sample. The doublet is related to the Co-rich phase having T_c below RT and therefore being paramagnetic at RT. The sextet results of the two magnetically ordered Fe-rich phases for which the Curie temperatures are above RT. The coexistence of the three spinel phases in the sample did not allow to determine the cationic distribution of each phase by the Mössbauer measurement carried out at 5 K under an external field of 60 kOe.

3.2.2. Sample annealed at 700 °C for 120 h (spinodal decomposition totally finished)

The sample $Co_{1.73}Fe_{1.27}O_4$ was annealed at 700 °C during 120 h in order to obtain complete spinodal decomposition [8,10].

The XRD pattern (Fig. 1c) confirms that the initial phase has vanished and that two new spinel phases have precipitated. To determine the composition of these two phases, the Rietveld method was used to refine the unit-cell parameter of each spinel phase. The results are given in Table 4. From these values and using Vegard's interpolation law between the end-members cobalt ferrite $CoFe_2O_4$ (a=8.392 Å) and cobalt oxide Co_3O_4 (a=8.08 Å), the composition of the Fe-rich and the Co-rich phases were determined to be $Co_{1.16}Fe_{1.84}O_4$ and $Co_{2.69}Fe_{0.31}O_4$, respectively. In accordance with these composition values, 62.8% of the Fe-rich phase and 37.2% of the Co-rich phase is necessary to obtain a mixture with a global composition of $Co_{1.73}Fe_{1.27}O_4$. These percentages are quite close to the proportions of 60% and 40%, respectively, as calculated by the Rietveld method.

The Mössbauer spectrum that has been acquired at RT after this annealing (Fig. 5) shows a doublet and sextet contribution. Clearly, the sextet arises from the magnetically ordered Fe-rich spinel phase for which the Curie temperature is much higher than RT. The doublet is related to the Co-rich phase having T_c below RT and therefore being paramagnetic at RT. Both phases (sextet and doublet) have a low isomer shift which is due to Fe^{3+}. It is expected that for the iron-rich phase the Fe^{3+} cations occupy both octahedral and tetrahedral sites, but that the two sextets strongly overlap and are not resolvable by the numerical analysis of the spectrum.

In the Mössbauer spectrum collected at 5 K with an external field of 60 kOe, the two spinel phases exhibit magnetic ordering and, as clearly illustrated in Fig. 5, the overall contributions from A- and B-sites are clearly shifted apart due to the external field. However, it is not possible to distinguish the two phases in the Mössbauer spectrum of their mixture. As mentioned before, the ferric cations exclusively occupy the B-sites of the cobalt-rich phase, and consequently cationic distribution in this phase may be written as $Co^{2+}_{1.00}[Fe^{3+}_{0.31}Co^{3+}_{1.69}]O^{2-}_4$

For the iron-rich phase the distribution formula is

$$Co^{2+}_{\alpha}Fe^{3+}_{1-\alpha}[Co^{2+}_{1-\alpha}Fe^{3+}_{0.84+\alpha}Co^{3+}_{0.16}]O^{2-}_4 \quad (3)$$

At first, it was considered that the involved applied-field Mössbauer spectrum is the result of three iron ions contributions: [Fe^{3+}] in A-sites of iron-rich phase, [Fe^{3+}] in B-sites of iron-rich phase and [Fe^{3+}] in B-sites of cobalt-rich phase. Indeed, Table 1 shows that the effective hyperfine field H_{eff} for octahedral ferric ions in an iron phase, is slightly different from the corresponding field for a cobalt-rich phase. Assuming three H_{eff} components, with initial values for H_{eff} of 563, 473 and 550 kOe for [Fe^{3+}] in A-sites of iron-rich phase, [Fe^{3+}] in B-sites of iron-rich phase and [Fe^{3+}] in B-sites of cobalt-rich phase, respectively, it was, however, not found possible to adequately fit the experimental spectrum with reasonable adjusted values of the various Mössbauer parameters. For that reason, the external-field spectrum was described by a superposition of only two magnetic components. The fitted values of some relevant spectral parameters are listed in Table 5.

In trying to obtain the cationic distribution of the iron-rich phase, the total iron content in A- and B-sites for both phases together was, in the frame of a first assumption, determined from the relative spectral areas R listed in Table 5. Cationic distribution

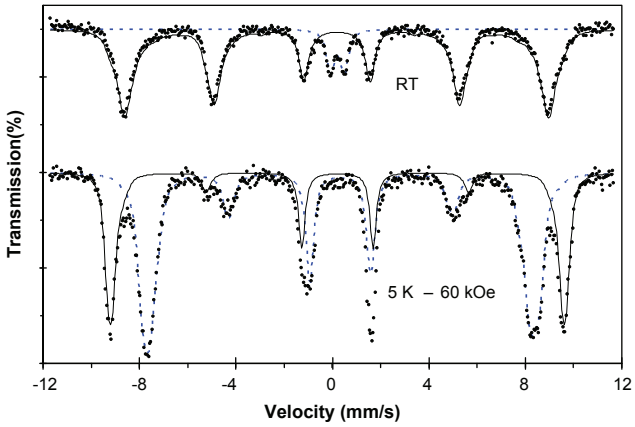

Fig. 5. Mössbauer spectra measured at 300 K and 5 K with an applied magnetic field of 60 kOe for $Co_{1.73}Fe_{1.27}O_4$ powder after spinodal decomposition by annealing at 700 °C for 120 h.

Table 5
Relevant Mössbauer parameters deduced from the spectrum recorded at 5 K in an external magnetic field (60 kOe) for $Co_{1.73}Fe_{1.27}O_4$ powder annealed for 120 h at 700 °C. H_{eff}: maximum probability effective hyperfine field, δ: isomer shift relative to α-Fe at room temperature and R: relative spectral area.

$Co_{1.73}Fe_{1.27}O_4$	A-sites			B-sites		
	δ (mm/s)	H_{eff} (kOe)	R (%)	δ (mm/s)	H_{eff} (kOe)	R (%)
Annealed at 700 °C/120 h	0.36	564	35.0	0.45	473	65.0

Table 4
Unit-cell parameter, composition and proportion of the phases obtained after spinodal decomposition at 700 °C for 120 h.

Global composition of the mixture	$Co_{1.73}Fe_{1.27}O_4$	
Phases	Fe-rich	Co-rich
Cell parameter (Å) (calculated by Rietveld refinement)	8.366(2)	8.128(2)
Proportion (mol%) determined from XRD refinement	60	40
Composition calculated with Vegard's law	$Co_{1.16}Fe_{1.84}O_4$	$Co_{2.69}Fe_{0.31}O_4$
Proportion (mol%) calculated to obtain a global composition of $Co_{1.73}Fe_{1.27}O_4$	62.8	37.2

in each oxide can then be deduced if the two-phase compound is assimilated to a mechanical phase mixture of the iron-rich and the cobalt-rich phases. Taking into account the global composition ($Co_{1.73}Fe_{1.27}O_4$), which contains 1.27 Fe^{3+} per unit formula, it is thus inferred that 0.44 Fe^{3+} are located in A-sites and 0.83 Fe^{3+} in B-sites. These amounts are shared between the two different phases.

All the Fe^{3+} cations (0.44 per formula unit of spinel) assigned to A-sites must be attributed to the iron-rich phase which represents 62.8% of the mixture. Hence, the number of Fe^{3+} cations per formula unit in the A-sites, for the phase $Co_{1.16}Fe_{1.84}O_4$, is 0.44/0.628 = 0.70, implying that the number of Fe^{3+} cations in the B-sites of the latter phase is 1.14. The cationic distribution of this phase is thus given by

$$Co^{2+}_{0.30}Fe^{3+}_{0.70}[Co^{2+}_{0.70}Fe^{3+}_{1.14}Co^{3+}_{0.16}]O^{2-}_4 \quad (4)$$

The as-such calculated amount of 0.7 Fe^{3+} cations in A-sites for the $Co_{1.16}Fe_{1.84}O_4$ phase is consistent with the cationic distribution deduced from the Mössbauer spectra of the single phased samples, listed in Table 3. Indeed, it is in between the values of 0.79 and 0.62 found for the compositions $Co_{1.00}Fe_{2.00}O_4$ and $Co_{1.22}Fe_{1.78}O_4$, respectively, even if oxides obtained after spinodal decomposition at 700 °C could have a lower inversion degree in comparison with the single phased reference samples annealed at 900 °C.

However, in view of the observed shift of the H_{eff} of Fe^{3+} in the cobalt-rich phase with respect to the results obtained for the corresponding single-phase spinel as reported above (see Table 1 and Fig. 3), a second consideration must be explored. Mentioned shift is such that the spectral contribution of Fe^{3+} cations in B-sites in the cobalt-rich phase actually closely overlaps with that of Fe^{3+} cations in A-sites for $Co_{1.16}Fe_{1.84}O_4$. That means that the aforementioned 0.44 Fe^{3+} cations per formula unit are distributed between the A- and B-sites of the iron- and cobalt-rich phases, respectively. Consequently, only 0.83 Fe^{3+} cations are then located in the B-sites of $Co_{1.16}Fe_{1.84}O_4$, instead of 1.14 as evaluated under the earlier assumption, implying that, taking into account the percentage of this phase, there are 0.83/0.628 = 1.32 Fe^{3+} cations in B-sites and 1.84–1.32 = 0.52 Fe^{3+} cations in A-sites. The structural formula according to this second assumption is then

$$Co^{2+}_{0.48}Fe^{3+}_{0.52}[Co^{2+}_{0.52}Fe^{3+}_{1.32}Co^{3+}_{0.16}]O^{2-}_4 \quad (5)$$

This cationic distribution seems to be inconsistent with the results obtained for the pure spinel phases studied in the first part of this work. According to these results, more than 0.6 Fe^{3+} cations are expected to be in A-sites.

Relevant magnetic data for the involved solid solutions are listed in Table 6. The total saturation magnetization of the oxides after the spinodal decomposition was calculated taking into account the M_S value and the percentage of each phase and was found to be 66.2 and 75.9 emu/g for assumption one and two, respectively. These values are significantly higher than that obtained experimentally by a SQUID measurement, i.e., 58.9 emu/g (see Fig. 6). This shortcoming is believed to be due to an overestimation of the value of M_S for the Co-rich phase as calculated according to the Néel model. As previously discussed, Takahashi and Fine [13] and Harrison and Putnis [22] showed that the real variation of M_S for Co concentrations exceeding the compensation point is lower than predicted by the Néel model (see Fig. 4). The value of M_S obtained from the second assumption, however, seems to be too remote from the experimental measurement, which can be possibly explained by a discrepancy from the Néel model of the magnetic behavior of the minority phase.

Even though the structural formulas (4) and (5) are relatively close, it seems, however, that composition (4) is more consistent with the results of the study of the pure spinel phases, on the one hand, and with the saturation magnetization measurement, on the other hand. This conclusion could infer that the effective field of the B-site Fe^{3+} ions of the iron cobaltite differs depending on whether the grains are (magnetically) isolated and independent

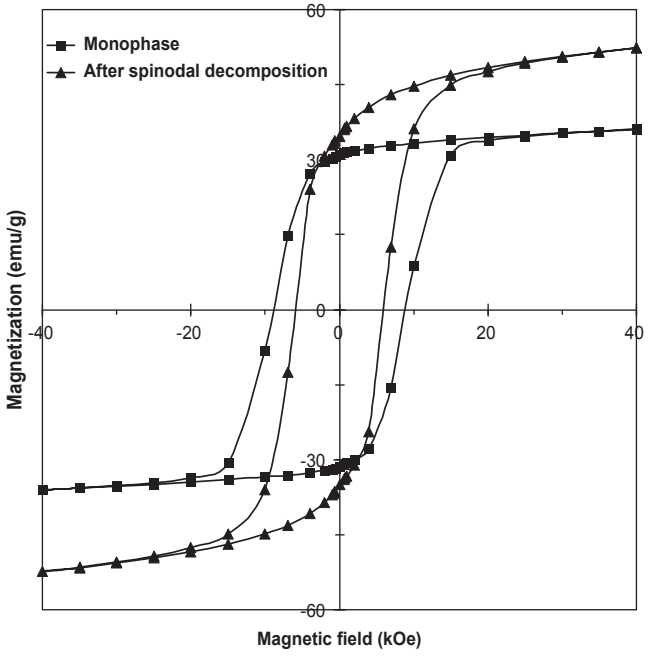

Fig. 6. Comparison of magnetic hysteresis loop measured at 5 K for pure $Co_{1.73}Fe_{1.27}O_4$ powder and after spinodal decomposition by annealing at 700 °C for 120 h.

Table 6
Cationic distribution deduced from Mössbauer spectra and comparison of calculated (at 0 K) and measured (at 5 K) magnetic properties after spinodal decomposition at 700 °C during 120 h.

$Co_{1.73}Fe_{1.27}O_4$	A-site		B-site			mol%	M_S cal. (emu/g)	M_S total cal. (emu/g)	M_S exp. (emu/g)
	Co^{2+} (3.2 μ_B)	Fe^{3+} (5 μ_B)	Co^{2+} (3.2 μ_B)	Fe^{3+} (5 μ_B)	Co^{3+} (0 μ_B)				
Pure phase annealed at 900 °C and quenched									
Monophase	0.61	0.39	0.39	0.88	0.73	100	–	40.9	39.3
After spinodal decomposition at 700 °C for 120 h (first solution)									
$Co_{1.16}Fe_{1.84}O_4$	0.30	0.70	0.70	1.14	0.16	62.8	82.6	66.2	58.9
$Co_{2.69}Fe_{0.31}O_4$	1.00	0.0	0.0	0.31	1.69	37.2	36.8		
After spinodal decomposition at 700 °C for 120 h (second solution)									
$Co_{1.16}Fe_{1.84}O_4$	0.48	0.52	0.52	1.32	0.16	62.8	98.2	75.9	58.9
$Co_{2.69}Fe_{0.31}O_4$	1.00	0.0	0.0	0.31	1.69	37.2	36.8		

or whether they are strongly linked to another magnetic phase (iron-rich phase).

Fig. 6 further shows that the spinodal decomposition leads to an increase of about 50% for the saturation magnetization and a decrease of the coercive field from 8910 Oe to 5350 Oe.

4. Conclusion

Iron cobaltite powders with compositions in between $CoFe_2O_4$ and $Co_{2.46}Fe_{0.54}O_4$ were synthesized. The cationic distribution of the pure spinel phases $Co_xFe_{3-x}O_4$ ($x=1.00$, 1.22, 1.73, and 2.46) was determined by Mössbauer spectroscopy. As the value of x increased, Co^{3+} cations replaced Fe^{3+} cations in the B-sites and Co^{2+} cations migrated from B-sites to A-sites. For $Co_{2.46}Fe_{0.54}O_4$, all the iron was located in octahedral sites. Saturation magnetizations M_S measured at 5 K were consistent with the values calculated from the cationic distribution according to the Néel model. M_S decreased as diamagnetic Co^{3+} cations replaced strongly magnetic Fe^{3+} cations. However, for $Co_{2.46}Fe_{0.54}O_4$ the experimental value of M_S was found slightly lower than the one calculated. For the values of x higher than 2.3, the relative increase in the magnetic moment of the A sublattice due to the increasing amount of diamagnetic Co^{3+} cations in B-sites makes the calculation by the collinear Néel model less suitable.

This single pristine phase was then submitted to subsequent thermal treatment in order to induce phase segregation by spinodal decomposition. The three-phase compound obtained at the intermediate state of the spinodal decomposition did not allow the determination of the cationic distribution of each phase by the Mössbauer measurement that was carried out at 5 K under an external field of 60 kOe.

After complete spinodal decomposition of the powder with the composition $Co_{1.73}Fe_{1.27}O_4$ two spinel phases were revealed. The iron-rich phase is $Co_{1.16}Fe_{1.84}O_4$ and the cobalt-rich one is $Co_{2.69}Fe_{0.31}O_4$. Cationic distribution of each oxide present in the two-phase mixture was then calculated using Mössbauer measurements of the pure $Co_xFe_{3-x}O_4$ phases ($x=1.00$, 1.22, 1.73, and 2.46) and of the mixture obtained after the decomposition. The increase in M_S value after the spinodal transformation was in accordance with the calculated value deduced from the cationic distribution of the two phases.

These results will be used in our future research work in which we want to achieve the spinodal decomposition of iron-cobaltites thin films.

References

[1] V. Gulyaev, S.A. Nikitov, L.V. Zhivotovskii, A.A. Klimov, Ph. Tailhades, L. Presmanes, C. Bonningue, C.S. Tsai, S.L. Vysotskii, Y.A. Filimonov, JETP Letters 77 (2003) 567–570.
[2] M.G.M. Miranda, E. Esteves-Rams, G. Martinez, M.N. Baibich, Physical Review B (2003)014434-1–014434-8.
[3] M.G.M. Miranda, A.T. da Rosa, R. Hinrichs, U. Golla-Schindler, A.B. Antunes, G. Martinez, E. Esteves-Rams, M.N. Baibich, Physica B 384 (2006) 175–178.
[4] A. Hutten, D. Sudfeld, K. Wojcrykowski, P. Jutzi, G. Reiss, Journal of Magnetism and Magnetic Materials 262 (2003) 23–31.
[5] J. Robin, Annales de Chimie 10 (1955) 389–412.
[6] M. Takahashi, M.E. Fine, Journal of American Ceramic Society 53 (1970) 633–634.
[7] M. Takahashi, J.R.C. Guimares, M.E. Fine, Journal of American Ceramic Society 54 (1971) 291–295.
[8] S. Hirano, T. Yogo, K. Kikuta, E. Asai, K. Sugiyama, H. Yamamoto, Journal of American Ceramic Society 76 (1993) 1788–1792.
[9] I.H. Jung, S. Decterov, A.D. Pelton, H.M. Kim, Y.B. Kang, Acta Materialia 52 (2004) 507–519.
[10] H. Le Trong, A. Barnabé, L. Presmanes, Ph. Tailhades, Solid State Sciences 10 (2008) 550–556.
[11] J. Rodriguez-Carvajal, Physica B 192 (1993) 55–69.
[12] R.D. Shannon, Acta Crystallographica A32 (1976) 751–767.
[13] M. Takahashi, M.E. Fine, Journal of Applied Physics 43 (1972) 4205–4216.
[14] R.E. Vandenberghe, E. De Grave, in: G.J. Long, F. Grandjean (Eds.), Mössbauer Spectroscopy Applied to Inorganic Chemistry, vol. 3, Plenum Press, New York, 1989 (Chapter 3).
[15] P.M.A. de Bakker, R.E. Vandenberghe, E. De Grave, Hyperfine Interactions 94 (1994) 2023–2027.
[16] P.A. Smith, C.D. Spencer, R.P. Stillwell, Journal of Physics and Chemistry of Solids 39 (1978) 107–111.
[17] R.E. Watson, A.J. Freeman, Physical Review 123 (1961) 2027–2047.
[18] E. De Grave, A. Van Alboom, Physics and Chemistry of Minerals 18 (1991) 337–342.
[19] S. Eeckhout, E. De Grave, Physics and Chemistry of Minerals 30 (2003) 142–146.
[20] G.A. Sawatzky, F. Van Der Woude, A.H. Morrish, Journal of Applied Physics 39 (1968) 1204–1206.
[21] G.A. Sawatzky, F. Van Der Woude, A.H. Morrish, Physical Review 187 (1969) 747–757.
[22] R.J. Harrison, A. Putnis, Surveys in Geophysics 19 (1999) 461–520.
[23] T.A.S. Ferreira, J.C. Waerenborgh, M.H.R.M. Mendonça, M.R. Nunes, F.M. Costa, Solid State Science 5 (2003) 383–392.
[24] P.J. Murray, J.W. Linnett, Journal of Physics and Chemistry of Solids 37 (1976) 1041–1042.